Can one identify the intrinsic structure of the yrast states in ^{48}Cr after the backbending?

Zao-Chun Gao,[1] Mihai Horoi,[2] Y. S. Chen,[1] Y. J. Chen,[1] and Tuya[3]
[1]*China Institute of Atomic Energy P.O. Box 275-10, Beijing 102413, China*
[2]*Department of Physics, Central Michigan University, Mount Pleasant, Michigan 48859, USA*
[3]*College of Physics Science and Technology, Shenyang Normal University, ShenYang 110034, China*
(Received 2 August 2010; revised manuscript received 13 April 2011; published 17 May 2011)

The backbending phenomenon in ^{48}Cr has been investigated using the recently developed projected configuration interaction (PCI) method, in which the deformed intrinsic states are directly associated with shell model wave functions. Two previous explanations, (i) $K = 0$ band crossing and (ii) $K = 2$ band crossing, have been reinvestigated using PCI, and it was found that both explanations can successfully reproduce the experimental backbending. The PCI wave functions in the pictures of $K = 0$ band crossing and $K = 2$ band crossing are highly overlapped. We conclude that there are no unique intrinsic states associated with the yrast states after backbending in ^{48}Cr.

DOI: 10.1103/PhysRevC.83.057303 PACS number(s): 21.60.Ev, 21.60.Cs, 21.10.Re, 27.40.+z

The backbending of ^{48}Cr was observed more than 10 years ago [1,2], but its interpretation remains controversial and challenging for the existing nuclear models. Shell model (SM) calculations have reproduced very well the yrast states of ^{48}Cr [3–5], but it is difficult to obtain physical insight because the laboratory frame wave function does not provide direct information associated with the deformed intrinsic structure. The cranked Hartree-Fock-Bogoliubov (CHFB) method is a complementary theory [6] often used to analyze the deformed intrinsic states. According to one CHFB analysis [4], ^{48}Cr is an axial rotor up to the backbending, after that the system changes to a spherical shape. An alternative and more detailed CHFB analysis [7] shows that the backbending of the ^{48}Cr is not associated with the single particle level crossing and that the intrinsic configuration remains unchanged.

The projected shell model (PSM) [8,9] is an alternative technique that mixes the best intrinsic SM configuration with other associated particle-hole configurations. The PSM analysis [10] indicates that the backbending in ^{48}Cr is due to a band crossing involving an excited four-quasiparticle (4-qp) band with $K = 2$, which represents a configuration of broken neutron and proton pairs. In addition, the same Ref. [10] uses the generator coordinate method (GCM) that provides the picture of a spherical band crossing, which in some sense is similar to the result of CHFB. It is said that the PSM needs 4-qp states to describe the spherical states with spin $I \geqslant 10$ [10]. However, a calculation of the overlap between the PSM wave function and the GCM wave function seems to be necessary.

In the present Brief Report, the backbending in ^{48}Cr is investigated in the framework of the newly developed method called projected configuration interaction (PCI) [11,12]. The PCI basis is built from a set of Slater determinants (SDs). Those SDs may have different shapes, including the spherical shape. Hence, the nuclear states with different intrinsic shapes can be mixed by the residual interaction. By using the same SM Hamiltonian, the PCI results can be directly compared with those of full SM calculations. Moreover, PCI uses deformed single-particle bases and, therefore, the physics insight of the results can be clearly analyzed. Different PCI bases can be built in such a way that they reflect the nature of the intrinsics states found in previous studies, such as CHFB (or GCM) and PSM. PCI wave functions were shown to be good approximations to those of full SM, and they can be obtained using different bases. Thereafter, overlaps among PCI wave functions can be calculated and analyzed to determine the validity of various explanations. These features suggest that PCI could shed new light on the interesting phenomenon of the backbending in ^{48}Cr. Other models using similar techniques includes the family of VAMPIR [13] and the quantum Monte Carlo diagonalization (QMCD) method [14].

For completeness we give here a brief introduction of the PCI method (see Refs. [11,12] for more details). The deformed single-particle (s.p.) states need to be generated from a deformed s.p. Hamiltonian that can be written as

$$H_{\text{s.p.}} = h_{\text{sph}} - \tfrac{2}{3}\epsilon_2\hbar\omega_0\rho^2 P_2 + \epsilon_4\hbar\omega_0\rho^2 P_4, \tag{1}$$

where $h_{\text{sph}} = \sum_i e_i c_i^\dagger c_i$ is the spherical s.p. Hamiltonian assumed to have the same eigenfunctions as the spherical harmonic oscillator and e_i energies are properly adjusted such that the SD with lowest energy is close to the HF vacuum. For the pf shell we use $e_{f_{7/2}} = 0.0$ MeV, $e_{p_{3/2}} = 4.5$ MeV, $e_{f_{5/2}} = 5.0$ MeV, and $e_{p_{1/2}} = 6.0$ MeV. In Eq. (1) ϵ_2, ϵ_4 are the quadrupole and hexadecapole deformation parameters, P_l are Legendre polynomials, $\rho = r/b$, and we take $b = 1.93$ fm for the harmonic oscillator parameter [3,4].

The SDs can be built with deformed s.p. states. Following our previous papers [11,12], the general structure of the PCI basis can be written as

$$\begin{Bmatrix} 0\text{p} - 0\text{h}, & n\text{p} - n\text{h} \\ |\kappa_1, 0\rangle, & |\kappa_1, j\rangle, \ldots, \\ |\kappa_2, 0\rangle, & |\kappa_2, j\rangle, \ldots, \\ \cdots & \cdots \\ |\kappa_N, 0\rangle, & |\kappa_N, j\rangle, \ldots \end{Bmatrix}, \tag{2}$$

where $|\kappa_i, 0\rangle$ $(i = 1, \ldots, N)$ is an optimal [12] set of starting states having different deformations. Assuming that these $|\kappa, 0\rangle$ are found (in what follows we skip the subscript i to

keep notation short), a number of relative np-nh SDs, $|\kappa, j\rangle$, on top of each $|\kappa, 0\rangle$ are added to the SD basis selected with the constraint [11]

$$\Delta E = \tfrac{1}{2}(E_0 - E_j + \sqrt{(E_0 - E_j)^2 + 4|V|^2}) \geqslant E_{\rm cut}. \qquad (3)$$

Here $E_0 = \langle\kappa, 0|H|\kappa, 0\rangle$, $E_j = \langle\kappa, j|H|\kappa, j\rangle$, and $V = \langle\kappa, 0|H|\kappa, j\rangle$. The PCI basis is then obtained by projecting the selected SDs onto good angular momentum. The wave functions, as well as the energy levels, are obtained by solving the following generalized eigenvalue equation:

$$\sum_{\kappa'} \left(H^I_{\kappa\kappa'} - E^I N^I_{\kappa\kappa'}\right) f^I_{\kappa'} = 0. \qquad (4)$$

Here $H^I_{\kappa\kappa'}$ and $N^I_{\kappa\kappa'}$ are given by

$$H^I_{\kappa\kappa'} = \langle\kappa|H P^I_{KK'}|\kappa'\rangle, \quad N^I_{\kappa\kappa'} = \langle\kappa|P^I_{KK'}|\kappa'\rangle, \qquad (5)$$

where $P^I_{KK'}$ is the angular momentum projection operator, and H is the SM Hamiltonian. In this study we take the KB3 interaction [15], which has been used by Caurier *et al.* in their SM calculations of ^{48}Cr [4].

Following the method described in Ref. [12], we first performed a "best" PCI calculation by setting $N = 15$ and $E_{\rm cut} = 0.5$ keV for all spins. The calculated energies, the $E2$ transition energies, and the $B(E2)$ values are compared with the full SM results in Fig. 1. The dimensions and the energy differences of the PCI and SM for each spin are listed in Table I. It is clear from Fig. 1 that the PCI results are very close to those of the full SM. All energy differences are less than 100 keV, indicating that all important correlations, including the $T = 1$ and $T = 0$ pairing, are properly taken into account.

To get a more clear insight into the structure of the states contributing to the backbending in ^{48}Cr, it is instructive to choose much smaller PCI basis, which is accurate enough and can be easily searched for the most important components. The analysis is also simplified if these smaller PCI bases are used to calculate all even-spin states from $I = 0$ to $I = 16$ using the method described in Ref. [11]. We chose two basic $|\kappa, 0\rangle$ SDs. The first $|\kappa_1, 0\rangle$ is a $K = 0$ configuration with all eight valence nucleons occupying the orbits with $|\Omega| = 1/2(1f_{7/2})$ and $|\Omega| = 3/2(1f_{7/2})$, as shown in Fig. 2(a). The

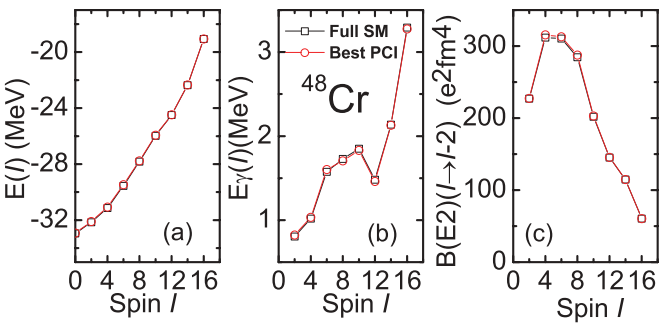

FIG. 1. (Color online) Results obtained with "best" PCI and full SM. (a) Yrast state energies vs spin. (b) $E2$ transition energy $E(I) - E(I-2)$ vs spin. (c) The $BE2$ values with the same wave functions as in (a). The effective charges are taken to be $1.5e$ for protons and $0.5e$ for neutrons, which are the same as those used in Refs. [3,4]. Results of the full SM are taken from Ref. [3].

TABLE I. The J-scheme dimensions and the energy differences of the best PCI and full SM.

Spin	Full SM dimension	Best PCI dimension	$E_{\rm PCI} - E_{\rm SM}$ (keV)
0	41 355	3949	25.75
2	182 421	4390	43.49
4	246 979	4845	58.85
6	226 259	5026	85.36
8	156 262	5168	61.58
10	83 247	5679	42.24
12	33 846	5302	21.22
14	10 095	2635	16.01
16	2038	1536	0.33

deformation of $|\kappa_1, 0\rangle$ is given by $\epsilon_2 = 0.19$ and $\epsilon_4 = -0.05$. This deformation was obtained by determining the minimum of the energy surface of $\langle K = 0|H_{\rm KB3}|K = 0\rangle$ as a function of ϵ_2 and ϵ_4 [see the dashed line in Fig. 2(b)]. A minimum energy of $\langle\kappa_1, 0|H_{\rm KB3}|\kappa_1, 0\rangle = -28.296$ MeV was found, which is close to the HF energy -28.423 MeV. $|\kappa_1, 0\rangle$ is believed to be responsible for the low-spin yrast states before the backbending, and the corresponding PCI basis that includes the np-nh states selected by Eq. (3) is denoted as "g.s." in Table II.

The second basic SD, $|\kappa_2, 0\rangle$, is chosen to describe the high spin states after the backbending. According to the previous studies mentioned in the Introduction, there are at least two candidate configurations for $|\kappa_2, 0\rangle$. First, as suggested by the CHFB calculations, the backbending can be explained without a band crossing [7], but by a shape change from large deformation to small deformation [4]. The calculations of the projected energy curves seem to be in good agreement with this interpretation. As one can see from Fig. 2(b) (solid lines), the deformation at minimum decreases as the spin increases. Guided by this result, one can establish a possible $|\kappa_2, 0\rangle$, which has the same configuration as $|\kappa_1, 0\rangle$, but whose shape is spherical. Such a choice of $|\kappa_2, 0\rangle$ SD would be consistent

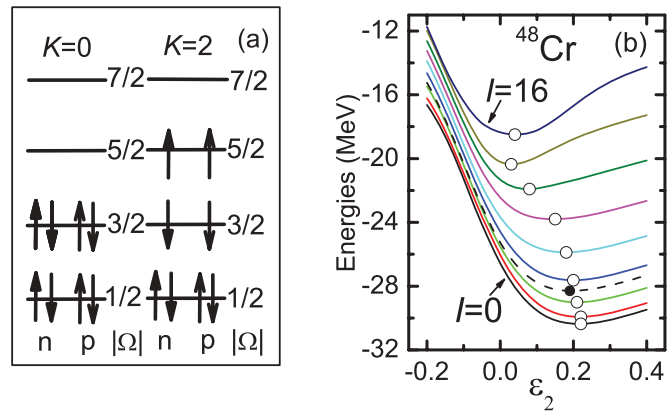

FIG. 2. (Color online) (a) The $K = 0$ and $K = 2$ configurations used in the present calculations of ^{48}Cr. All four levels are from $1f_{7/2}$ subshell. (b) Potential energy curves of the $K = 0$ configuration in (a) as functions of ϵ_2. The solid lines show the projected energies and the dashed line shows unprojected energy. ϵ_4 was chosen to minimize the potential energy for each ϵ_2. KB3 interaction was used.

TABLE II. PCI bases used for the backbending study in ^{48}Cr. $K = 0$ and $K = 2$ configurations are shown in Fig. 2.

Basis	g.s.			A			B			C		
	K	ϵ_2	ϵ_4	K	ϵ_2	ϵ_4	K	ϵ_2	ϵ_4	K	ϵ_2	ϵ_4
$\|\kappa, 0\rangle$	0	0.19	−0.05	0	0.00	0.00	2	0.00	0.00	2	0.19	−0.05
D_κ		143			192			366			280	

with the GCM interpretation. One should recall that in the PSM interpretation [10], the backbending in ^{48}Cr is caused by a $K = 2$ band crossing. Therefore, PCI seems to be ideally suited to include and analyze another possible $|\kappa_2, 0\rangle$ with $K = 2$. Its configuration is also shown in Fig. 2(a), and its structure can be chosen either spherical (see column B in Table II) or of the same deformation as that of $|\kappa_1, 0\rangle$ favored by the PSM approach (see column C in Table II). In an attempt to find the optimal structure of yrast states in ^{48}Cr after the backbending, we considered all three possibilities of $|\kappa_2, 0\rangle$, labeled with A, B, and C in Table II.

The np-nh $|\kappa,\ j\rangle$ SDs built on top of each $|\kappa, 0\rangle$ are selected by setting $E_{\rm cut} = 0.5$ keV in Eq. (3). Consequently, the number of selected $|\kappa_1,\ j\rangle$ is 142, and those of $|\kappa_2,\ j\rangle$ for A, B, and C are 191, 365, and 279, respectively. Adding the $|\kappa, 0\rangle$ itself, the total number of the selected SDs, D_κ, for each $|\kappa, 0\rangle$ is listed in Table II.

The calculated lowest energies with basis g.s., A, B, and C as functions of spin are shown in Fig. 3(a). The g.s. band is very smooth, without exhibiting any backbending. For the bases A, B, and C, all the corresponding energy curves cross the g.s. band around spin $I = 10$. At $I = 10$, the lowest energy is provided by basis C. This indicates that PSM is more reasonable in describing the band-crossing region. The overlaps between corresponding wave functions are shown in Fig. 4(a). The large overlaps indicate that quite different intrinsic bases would generate almost the same wave functions after the angular momentum projection.

The $E_\gamma(I) = E(I) - E(I-2)$ energies calculated using combinations of bases g.s. + A, g.s. + B, and g.s. + C are shown in Fig. 3(b). The backbending phenomenon seems to be easily reproduced by all these bases. As already discussed, the g.s. + A basis is qualitatively similar to that used in the CHFB and GCM analyses, while the g.s. + C basis follows the scenario proposed by the PSM analysis. More importantly, as shown in Fig. 4(b), the overlaps $|\langle\Psi_{\rm g.s.+A}(I)|\Psi_{\rm g.s.+C}(I)\rangle|$ are at least 92%. For the first time, the equivalence of the CHFB and PSM explanations has been confirmed. One should note, however, that the backbending described with the g.s. + C basis is quantitatively not as good as that described with the g.s. + A basis. The reason could be the large deformation of C basis. Changing the deformation of C basis to spherical, one gets the g.s. + B basis, and the result is improved. This feature supports the idea that the shape of ^{48}Cr reduces after backbending, as has been pointed out in Refs. [4,7].

Notice that the results with bases g.s. + A and g.s. + B are almost identical, although the bases A and B have completely different structures. Our calculations show that there are also other intrinsic bases with K different than 0 and 2 that can reproduce the backbending, and whose corresponding wave functions are almost equivalent to those with the basis g.s. + A or g.s. + B. In other words, one cannot find a unique intrinsic state for the yrast states in ^{48}Cr for $I = 12-16$. One can get some insight into the apparent irrelevance of the intrinsic structure at high spins by analyzing the case of $I = 16$, which is a band termination state. In the space of $\pi 1f_{7/2}^4 \nu 1f_{7/2}^4$, there is only one SD that reaches the maximum $K = 16$, showing that only one $I = 16$ state can be constructed. However, many $\pi 1f_{7/2}^4 \nu 1f_{7/2}^4$ SDs with various K values can be projected onto good I, and we have many projected states with $I = 16$, which are exactly identical and the projected energy is −18.342 MeV for the KB3 interaction. Therefore, one can use any one of the $\pi 1f_{7/2}^4 \nu 1f_{7/2}^4$ SDs to represent the state of band termination.

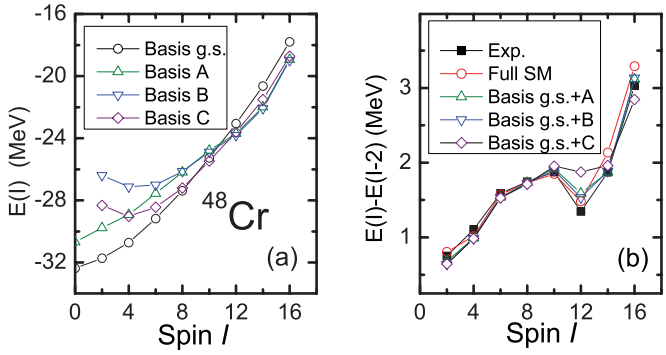

FIG. 3. (Color online) (a) PCI energies $E(I)$ as functions of spin for the bases listed in Table II. (b) $E2$ transition energies $E(I) - E(I-2)$ vs spin I. Experimental data are taken from Ref. [2].

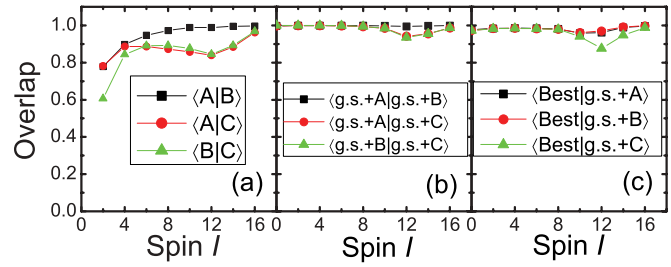

FIG. 4. (Color online) (a) Overlaps among the PCI wave functions for bases A, B, and C. Here $\langle A|B\rangle$ is the abbreviation of $|\langle\Psi_A(I)|\Psi_B(I)\rangle|$, and the same for the others. (b) Overlaps among the PCI wave functions for basis sets g.s. + A, g.s. + B, and g.s. + C. (c) Overlaps between the best PCI wave functions and those for basis sets g.s. + A, g.s. + B, and g.s. + C.

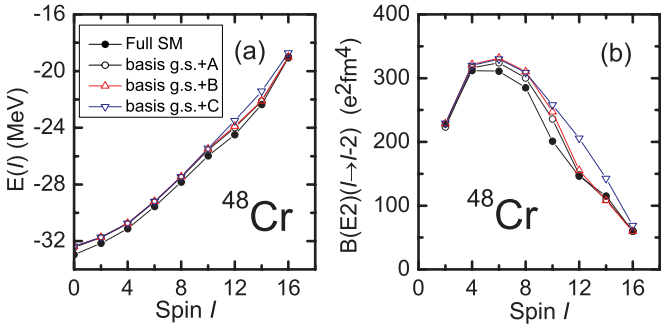

FIG. 5. (Color online) (a) Yrast state energies vs spin obtained with PCI (open symbols) and full SM (solid symbols). (b) The $BE2$ values with the same wave functions as in (a). Results of the full SM are taken from Ref. [3].

Calculation of the overlap between the PCI and the full SM wave function is very difficult because the number of the norm matrix elements, $N_{\rm PCI} \times N_{\rm SM}$, is huge. Here $N_{\rm PCI}$ and $N_{\rm SM}$ are dimensions of the PCI and the full (M-scheme) SM spaces. However, Fig. 1 and Table I clearly show that the best PCI calculations are almost identical to the full SM results. Therefore, we assume that the best PCI wave functions can be regarded as replacements of the full SM wave functions. Overlaps between the best PCI wave functions and those for basis sets g.s. + A, g.s. + B, and g.s. + C are given in Fig. 4(c). One can see that the overlaps are generally large. This fact clearly shows that the most important physics of the yrast states in ^{48}Cr has been incorporated into the PCI wave functions with a very small basis. Therefore, the PCI energies and the $B(E2)$ values should be relatively close to those of the exact values, and the results are shown in Fig. 5. With only a small fraction of the best PCI dimension, the PCI energies obtained with bases g.s. + A, g.s. + B, and g.s. + C are, on average, only few hundred keV above the exact values. For the $B(E2)$ calculations, we used the same effective charges as in Refs. [3,4]. The $B(E2)$ values looks also close to the exact ones.

In summary, the backbending in ^{48}Cr has been studied with a recently developed PCI method. PCI uses the same realistic Hamiltonians and valence spaces as the SM calculations, but only a set of properly selected SDs with different deformations and associated np-nh configurations. The backbending in ^{48}Cr has been reproduced by using various PCI bases, carefully selected to reflect the physics of the apparently different intrinsic states found by the CHFB (GCM) and PSM analyses of this case. Using the PCI capabilities of mixing these bases we confirm for the first time that the backbending pictures proposed by the CHFB and PSM methods are qualitatively equivalent. Our analysis supports the conclusion that there is no unique intrinsic state for spins larger than 10 in ^{48}Cr.

This work is supported by the NSF of China Contract No. 10775182. Z.G. and M.H. acknowledge support from the US DOE UNEDF Grant No. DE-FC02-09ER41584. M.H. acknowledges support from NSF Grant No. PHY-0758099. Y.S.C. acknowledges support from the MSBRDP of China under Contract No. 2007CB815003.

[1] J. A. Cameron *et al.*, Phys. Rev. C **49**, 1347 (1994).
[2] J. A. Cameron *et al.*, Phys. Lett. B **387**, 266 (1996).
[3] E. Caurier, A. P. Zuker, A. Poves, and G. Martinez-Pinedo, Phys. Rev. C **50**, 225 (1994).
[4] E. Caurier *et al.*, Phys. Rev. Lett. **75**, 2466 (1995).
[5] F. Brandolini and C. A. Ur, Phys. Rev. C **71**, 054316 (2005).
[6] P. Ring and P. Schuck, *The Nuclear Many-Body Problem* (Springer-Verlag, Berlin, 1980).
[7] T. Tanaka, K. Iwasawa, and F. Sakata, Phys. Rev. C **58**, 2765 (1998).
[8] K. Hara and Y. Sun, Int. J. Mod. Phys. E **4**, 637 (1995).
[9] Y. S. Chen and Z. C. Gao, Phys. Rev. C **63**, 014314 (2000).
[10] K. Hara, Y. Sun, and T. Mizusaki, Phys. Rev. Lett. **83**, 1922 (1999).
[11] Z.-C. Gao and M. Horoi, Phys. Rev. C **79**, 014311 (2009).
[12] Z.-C. Gao, M. Horoi, and Y. S. Chen, Phys. Rev. C **80**, 034325 (2009).
[13] K. W. Schmid, Prog. Part. Nucl. Phys. **52**, 565 (2004).
[14] M. Honma, T. Mizusaki, and T. Otsuka, Phys. Rev. Lett. **77**, 3315 (1996).
[15] A. Poves and A. P. Zuker, Phys. Rep. **71**, 141 (1981).